COMPARISON BETWEEN FAULT ARCHITECTURE AND LABORATORY EXPERIMENTS IN THE MAIN ETHIOPIAN RIFT: IMPLICATIONS FOR RIFT MATURITY

[1]A. Agostini, [2]M. Bonini, [2]G. Corti, [1]F. Sani

[1]Dept. of Earth Sciences, Florence University, Florence, Italy

[2]Institute Geosciences and Earth Resources, CNR, Florence, Italy

The MER is part of the largest East African Rift System (EARS), a region of rifting that accommodates the active extension between the major Nubia and Somalia Plates (e.g. Ebinger, 2005; Corti, 2009). The MER extends from the Afar triple junction to the North, to the northern Kenya Rift to the South (Fig. 1). This area offers a complete record of the time-space evolution of a continental rift and thus represents a key area where analysing the characteristics of the rifting process.

The MER is traditionally differentiated into three main segments differing in terms of rift trend, fault patterns and lithospheric characteristics (Fig. 1; e.g. Mohr, 1983; Hayward and Ebinger, 1996; Bonini et al., 2005): (1) the ~N50°-55°E-trending Northern MER (NMER), (2) the ~N30°-40°E Central MER (CMER), and (3) the Southern MER (SMER) further subdivided into two sub-segments: (3a) a ~N20°-25°E-trending northern sub-segment (SMERn) and (3b) a ~N0°-10°E-trending southern sub-segment (SMERs).

The different MER segments are characterised by two distinct systems of normal faults that differ in terms of orientation, structural characteristics (e.g. length, vertical throw), timing of activation and relation with magmatism: (1) a Late Miocene-Pliocene system of border faults and (2) a set of Late Pliocene(?)-Quaternary faults affecting the rift floor, usually referred to as Wonji Fault Belt (e.g. Boccaletti et al., 1998). In this paper we have characterised the brittle deformation in different segments of the rift, through the statistical analysis of a new database of faults obtained from the integration satellite images and digital elevation models, and implemented with field controls. The remote sensing analysis allowed recording 3302 structures spanning in length, from ~100 m to 75 km (Fonko fault) on the western border of the Central MER (Fig. 1).

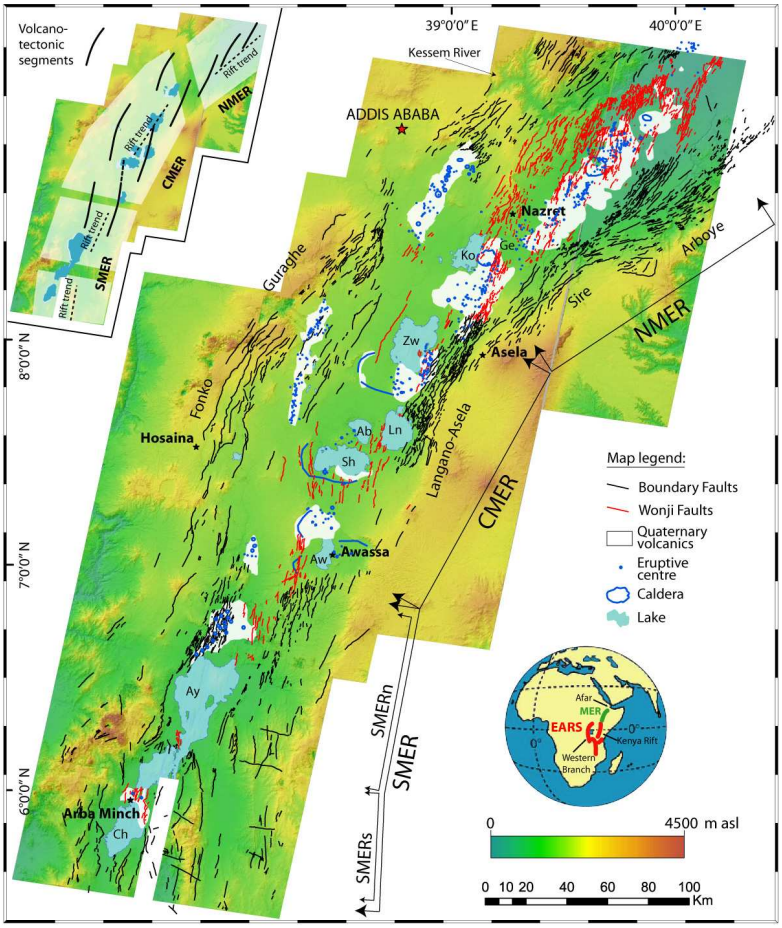

Figure 1 New database of faults of the Main Ethiopian Rift superimposed onto a digital elevation model obtained from the elaboration of the Aster images (see text for details). NMER, Northern MER; CMER, Central MER; SMER, Southern MER (SMERn, northern subsegment; SMERn, southern subsegment). The small inset to top-left hand side shows the en-echelon right stepping arrangement of the volcano-tectonic Wonji Fault Belt segments (from Corti, 2009), and the different MER segments. Ko: Lake Koka; Ge: Gedemsa Caldera; Zw: Lake Ziway; Ln: Lake Langano; Ab: Lake Abyata; Sh: Lake Shala; Aw: Lake Awasa; Ay: Lake Abaya; Ch: Lake Chamo.

Statistical analyses of these faults were carried out for each MER segment. In the NMER, the internal WFB faults, organized in en-echelon segments, are higher in number than the border faults (Fig. 2). The border faults consist

of long and spaced en-echelon structures (average length 1.80 km, maximum length ~25 km, average spacing 1035 m), whereas the internal faults are shorter (average length 1.26 km, maximum length ~15km) and more closely spaced (955 m on average). In the CMER and SMER border faults predominate onto internal faults (Fig. 2). Moreover border faults are longer (2.56 km and 2.64 km in the CMER and in the SMER, respectively) and more spaced (1200 m and 1260 m in the CMER and SMER, respectively) compared with the northern segment. Qualitatively, the internal faults in the CMER and SMER segments appear as short structures (only a few faults are longer than 10 km) with small vertical separation (e.g. Boccaletti et al., 1998), resulting individually similar to those in the NMER (Fig. 1).

Fault trace orientation was also analyzed in term of azimuthal distribution in the different rift segments. In the roughly ~N50°-55°-trending NMER, the total fault azimuth histogram shows a main peak trending between N20° and N25° (Fig. 2). This peak corresponds to the orientation of the WFB faults. The border faults are instead characterized by a main peak at ~N35°-40°, which is thus slightly oblique to the rift trend (Fig. 2). The ~N30°-40°-trending CMER shows a main peak varying between N25° and 30°, which corresponds to the border faults system. The WFB faults in the CMER are obviously less expressed than in the NMER (compare the height of the peaks in the corresponding histograms in Fig. 2) and exhibit a N10°-N15°- trending main peak. The analysis of the fault distribution in the SMER considered the subdivision into the ~N20°-25°-trending SMERn and the roughly ~N0°-10°-trending SMERs. In the SMERn, the border faults show a main peak varying between N20° and N25°, whereas in the SMERs the border fault peak trends ~N10°-15° (Fig. 2). In both sub-segments, the peaks of internal faults are oriented ~N10°-15°, although their importance is marginal. The analysis of the fault azimuth distribution in the different MER segment histograms reveals that the angle between the internal and border faults decreases from the NMER (~20°) southwards (~15° in CMER and SMERn), reaching a semi-parallelism between the two fault systems in the SMERs.

Statistical analysis on fault systems has been compared with the results of lithospheric-scale analogue models reproducing the kinematical conditions of orthogonal and oblique rifting (Agostini et al., 2009). Analogue models were performed in an artificial gravity field of ~18g by using a large capacity centrifuge. The models reproduced the extension of a 50km-thick continental lithosphere (crust+lithospheric mantle) floating above a low viscosity material simulating the asthenosphere (see Corti, 2008); the models were made of sand powder and silicone mixtures to reproduce the brittle and ductile behaviour of lithospheric layers. The experimental lithosphere contained a central weakness zone, analogous to the presence of a pre-existing weakness zone in nature that localizes deformation during progressive extension. Varying the orientation of the this weakness with respect to the extension direction allowed controlling rift kinematics. The adopted model to nature length ratio was 6.7×10^{-7}, such that 1 cm in the model corresponded to ~15 km in nature. More details about the modelling approach are described in Agostini et al. (2009). We summarize the four models that best fit the MER segments in terms of fault pattern and rift architecture (Fig. 3). These models vary from pure orthogonal extension (α=0°, being α the angle between the orthogonal to the pre-existing weakness and the direction of extension), to low (α=15° and α=30°) and moderate obliquity (α=45°). In all the models, rift evolution consisted of two distinct evolutionary stages, each characterized by the development of a peculiar fault system. The first evolutionary stage was characterized by basin subsidence and activation of large, en-echelon boundary faults parallel to the rift trend for α=0°, and slightly oblique for low to moderate obliquity (main orientation peak ~10-15° for α=15°, ~15-20° for α=30°, and ~20°-25° for α=45°; Fig. 3). Antithetic faults developed in the rift depression defining a couple of marginal grabens (whose expression became less clear increasing α) delimiting an undeformed rift floor. In this first stage all the deformation was accommodated along the rift margins by slip on the border and antithetic faults As extension proceeded incipient faults appeared on the relatively undeformed rift depression testifying a migration of deformation from the rift borders toward the rift centre. For increasing extension, internal faults increasingly accommodated deformation and the activity of boundary faults consequently reduced. This behaviour characterizes the second evolutionary phase. In orthogonal extension and low obliquity models (α from 0° to 30°), the internal faults developed during the second stage were orthogonal to the extension direction (main orientation peak around N0°-05°), whereas these faults were slightly oblique in moderate obliquity models (peak around N10°-15°)
In low and moderate obliquity model the internal faults were arranged in two en-echelon segments linked by a complex transfer zones, where rift-parallel faults were observed. For α=30° and α=45° the last extension steps led the internal faults to further propagate and interact with the rift margins, acquiring a S-shape geometry to adjust with the border faults.

The peculiar distribution and architecture of faulting in the different MER segments (Fig. 1) can be associated with different obliquity models; specifically, the NMER can be compared to the α=45° model, the CMER to the α=30° model, and the SMERn and SMERs to the α=15° and orthogonal extension models, respectively (Fig. 3).

The main points of similarity between the rift architecture in models and in the different MER segments are:
1) The analogue models and natural prototype display similar fault patterns, characterized by the two distinct fault families affecting the margins and the rift depression (Corti, 2008). Both in models and nature, the two fault systems are normally arranged into right-stepping en-echelon segments, suggesting a strike-slip component of displacement.
2) The two-stage model evolution mimics the diachronous activation of border faults and internal Wonji faults during the Late Miocene-Early Pliocene and Late Pliocene(?)-Early Pleistocene, respectively (at least in the NMER).
3) The main fault orientation peaks in each analogue model (α varying from 0° to 45°) are best fitted to the fault peaks in the corresponding MER segment after an invariable 10° clockwise rotation (Figs. 2, 3). The internal faults orientation display an equivalent along-axis variability controlled by the α angle both in models and nature. Particularly, they are

perpendicular to the inferred direction of extension in the CMER and SMER, as well as in the corresponding low-obliquity (α =15°-30°) and orthogonal (α =0°) models, whereas they trend oblique in the NMER and in the 45°-obliquity model, forming a ~10°-15° angle with the orthogonal to the stretching vector (Fig. 2).

4) In moderate obliquity models (α=45°) inward migration of deformation occurs at the early stages of extension, implying that internal faults increasingly accommodates the extensional strain and the border faults are progressively deactivated. Analogously, in the NMER the main fault peak corresponds to the WFB that dominantly accommodate extension, whereas the border faults are characterised by a lower statistical weight being them largely inactive and eroded, as indicated by geological data and historic and current seismicity (Wolfenden et al., 2004; Keir et al., 2006). Conversely, in models with α≤30° later inward migration of faulting implies that border faults accommodate a significant portion of deformation throughout the model evolution. This accords with the higher statistical weight of the border faults over the WFB in the CMER and SMER, where seismicity data indicates the border faults to be tectonically active (Keir et al., 2006).

5) Both in the MER and in the models, the angle between internal and border faults is a function of the rift trend (i.e., the rift obliquity), and this angle increases as the obliquity angle α increases. Moreover, both MER segments and models show a similar dependence of the total span of fault orientation on rift obliquity, showing the fault azimuth spectrum an overall increase with increasing α value.

6) The length of model boundary faults increases from α=45° to α=0° and, in a similar fashion, border fault length increases from the NMER to the SMER.

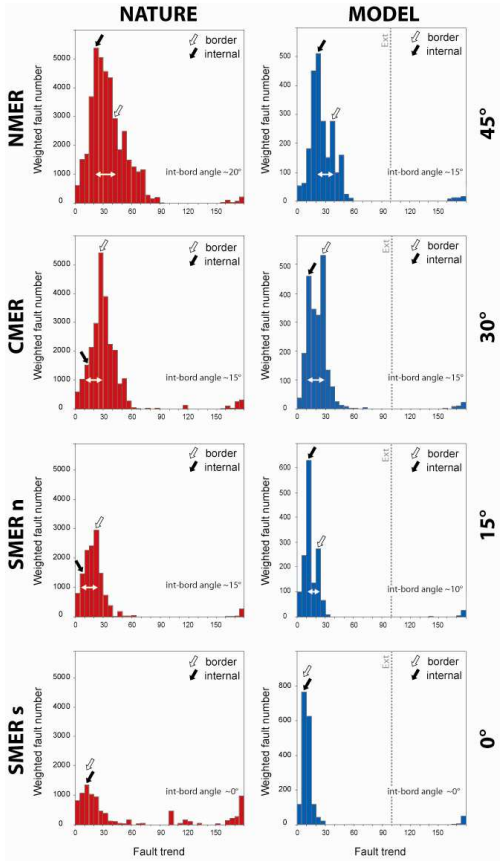

Figure 2. Main Ethiopian Rift (left column) versus model (right column) fault azimuth distribution. Note that the fault azimuth distribution of models has been rotated 10° clockwise to achieve the best fit with the corresponding MER segments. The white horizontal doublehead arrows indicate the angle between internal and border faults.

Integration of these approaches suggests substantial differences in fault architecture in different rift segments that in turn reflect an along-axis variation of the rift evolution and southward decrease in rift maturity (Fig. 4). The northernmost segment (Northern MER) is in a stage of incipient continental rupture in which deformation is localised within the rift floor along discrete tectono-magmatic segments and the boundary faults are almost inactive. The central MER sector records a transitional stage in which migration of deformation from boundary faults to faults internal to the rift valley is in an incipient stage. The southernmost MER is instead in an early continental stage, with the largest part of deformation accommodated by boundary faults and almost absent internal faults. The MER thus records along its axis the typical evolution of continental rifting, from fault-dominated rift morphology in the early stages of extension toward magma-dominated extension during break-up.

The extrapolation of modelling results suggests that oblique rifting conditions have been controlling the MER evolution since its birth in the Late Miocene, related to a constant post ca. 11 Ma ~N100°E Nubia-Somalia motion. The

current analysis highlights the major role played by the oblique extensional kinematics in controlling the rift architecture and the progression of rift evolution.

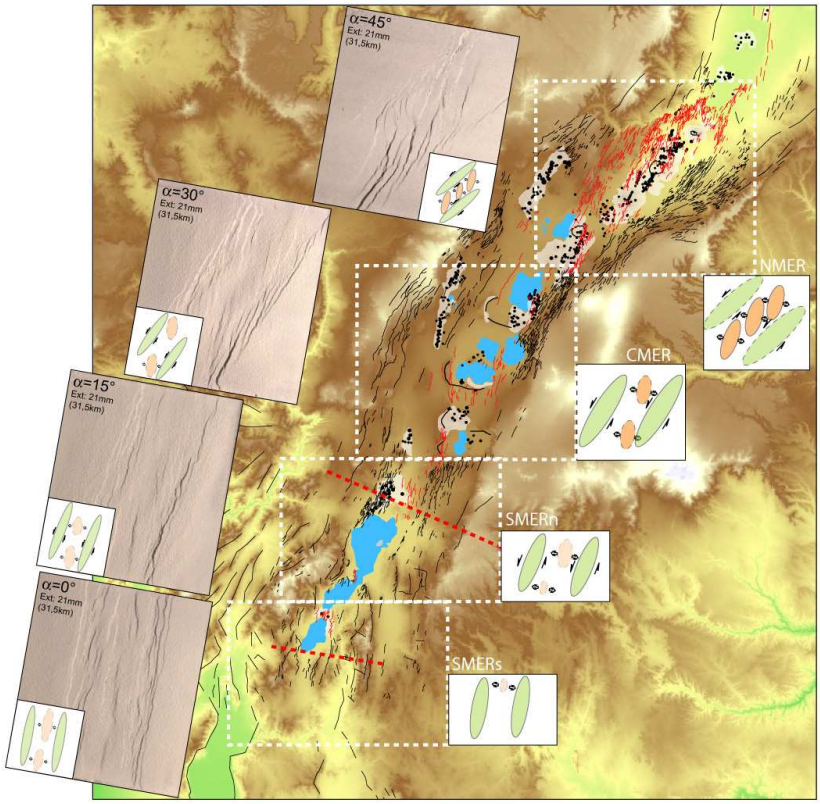

Figure 3. Comparison of fault pattern and rift architecture in models and the different correlative MER segments. Model top-views are rotated 10° clockwise to match the rift trend in the corresponding MER segments. Note the similarity in rift architecture.

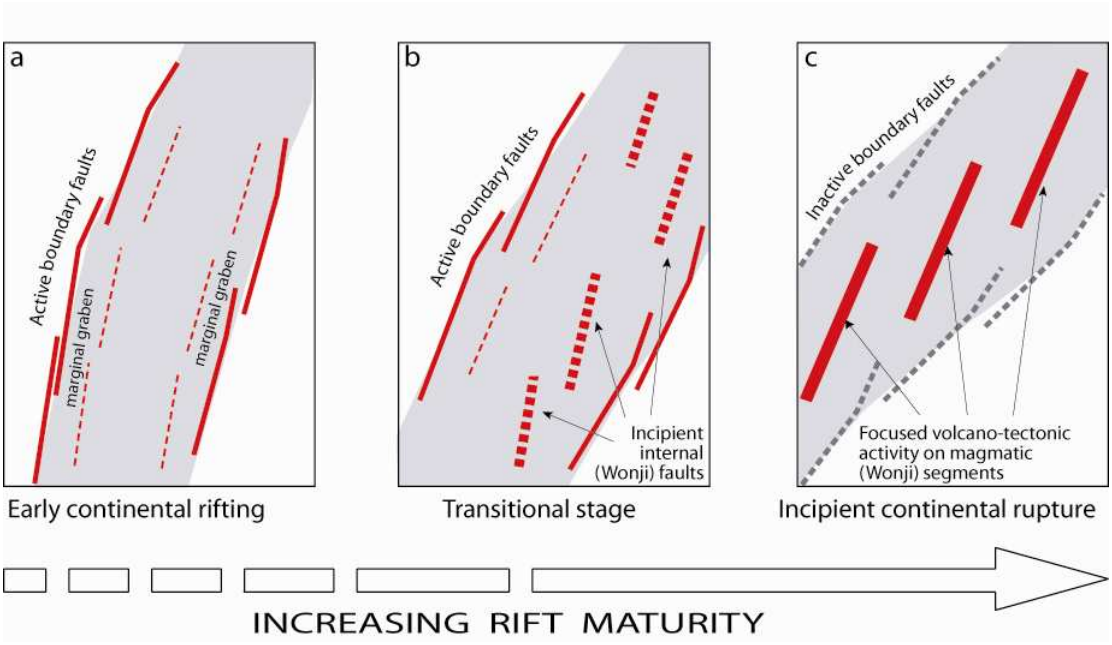

Figure 4. Idealised schematic evolution of a continental rift based on the comparison between structural analysis of the MER and the analogue model results. Each MER segment is exemplificative of a specific evolutionary rifting stage: (a) early continental rifting stage with active boundary faults and marginal grabens defining a subsiding essentially undeformed basin (i.e., SMER); (b) transitional stage characterized by active boundary faults and incipient internal faults starting to affect the rift valley floor (i.e., CMER); (c) incipient continental rupture stage where deformation is mainly accommodated by volcano-tectonic segments inside the rift depression (i.e., NMER).